Click-modified hexahomotrioxacalix[3]arenes as fluorometric and colorimetric dual-modal chemosensor for 2,4,6-trinitrophenol

Chong Wu,[a] Jiang-Lin Zhao,[a] Xue-Kai Jiang,[a] Xin-Long Ni,[b] Xi Zeng,[b] Carl Redshaw[c] and Takehiko Yamato*[a]

[a] Department of Applied Chemistry, Faculty of Science and Engineering, Saga University, Honjo-machi 1, Saga 840-8502, Japan

[b] Key Laboratory of Macrocyclic and Supramolecular Chemistry of Guizhou Province, Guizhou University, Guiyang 550025, People's Republic of China

[c] Department of Chemistry, The University of Hull, Cottingham Road, Hull, Yorkshire, HU6 7RX, UK

ABSTRACT: A new type of chemosensor-based approach to the detection of 2,4,6-trinitrophenol (TNP) is described in this paper. Two hexahomotrioxacalix[3]arene-based chemosensors **1** and **2** were synthesized through click chemistry, which exhibited high binding affinity and selectivity toward TNP as evidenced by UV-vis and fluorescence spectroscopy studies. ^{1}H NMR titration analysis verified that CH···O hydrogen bonding is demonstrated as the mode of interaction, which possibly facilitates effective charge-transfer.

Keywords: Hexahomotrioxacalix[3]arene, Click chemistry, Colorimetric chemosensor, Fluorometric chemosensor, 2,4,6-Trinitrophenol.

* Corresponding author. Fax: +81 952 28 8548.
E-mail address: yamatot@cc.saga-u.ac.jp (T. Yamato).

Graphical Abstract

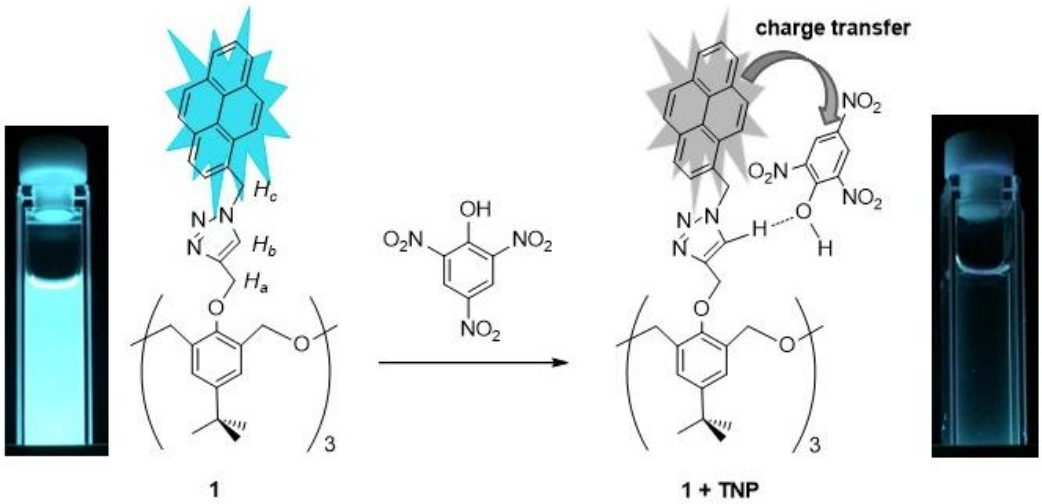

Highlight:

➢Click-modified hexahomotrioxacalix[3]arene is developed for the first time to detection TNP.

➢Fluorometric and colorimetric dual-modal chemosensor for TNP.

➢Highly selective and sensitive are obtained and the detection limit is 70 ppb.

➢A novel design strategy for developing chemosensors for TNP has been demonstrated.

1. Introduction

The design of chemosensors that are able to selectively recognize and sense specific analytes is an attractive research area in supramolecular chemistry [1-4]. In particular, the rapid and accurate detection of nitro-containing explosives is a high priority for security and health/environmental issues [5-6]. Various analytical techniques such as gas chromatography coupled with different detectors [7,8], high performance liquid chromatography [9,10], ion-mobility spectroscopy [11,12], Raman or surface enhanced Raman spectroscopy [13,14], electrochemical methods [15,16] and fluorescence spectroscopy [17,18] have been used for the detection of nitro-containing explosives. Among these techniques, fluorescence-based detection offers several advantages over other analytical methods with respect to high sensitivity, specificity, and real-time monitoring with fast response times [19]. To date, considerable effort has been devoted to the development of fluorescence sensing materials to detect nitro-containing explosives [20,21]. Even though several π-conjugated polymers [22] and metal-organic frameworks [23] have been employed to detect nitro-containing explosives, the development of reliable and efficient organic chemosensors possessing high selectivity for nitro-containing explosives remains a very challenging task [24,25].

Calixarenes are ideal frameworks for the development of chemosensors in the molecular recognition of chemical and biological targets of interest since the incorporation of a suitable sensory group into the calixarene results in a tailored

chromogenic receptor [26,27]. In particular, since Sharpless et al. developed click chemistry as a new coupling strategy in 2001 [28], numerous calixarene derivatives incorporating click-derived triazoles have been reported, which can be used as metal ions chemosensors via coordination at nitrogen atom [29-31]. However, these fluorescence systems have scarcely been exploited for the sensing of nitro-containing explosives. As a matter of fact, given the strong dipolar character of the triazole ring, the C–H bond of the heterocycle makes a surprisingly good hydrogen bond donor [32,33]. On the other hand, nitro-containing explosives often act as good electron acceptors due to the presence of electron withdrawing nitro ($-NO_2$) group/s [34]. Considering these two opposite properties of triazole and nitro-containing explosives, one might consider if noncovalent interactions exist between them?

In molecular recognition processes, noncovalent interactions such as hydrogen bonding, aromatic π-stacking and weak intermolecular interactions play a crucial role. With this in mind, can we utilize the click-derived triazole to design chemosensors for nitro-containing explosive sensing? Herein, we report two triazole-modified hexahomotrioxacalix[3]arenes **1** and **2** as a new type of chemosensor for the selective detection of 2,4,6-trinitrophenol (TNP) explosive. To the best of our knowledge, this is the first report where a triazole-modified hexahomotrioxacalix[3]arene serves as a selective chemosensor for TNP.

2. Experimental section

2.1. General

Unless otherwise stated, all reagents were purchased from commercial sources and used without further purification. All solvents were dried and distilled by the usual procedures before use. Melting points were determined using a Yanagimoto MP-S1. ^{1}H NMR and ^{13}C NMR spectra were recorded on a Nippon Denshi JEOL FT-300 NMR spectrometer and a Varian-400MRvnmrs400 with $SiMe_4$ as an internal reference: *J*-values are given in Hz. IR spectra were measured as KBr pellets or as liquid films on NaCl plates in a Nippon Denshi JIR-AQ2OM spectrophotometer. UV spectra were measured by a Shimadzu UV-3150UV-vis-NIR spectrophotometer. Fluorescence spectroscopic studies of compounds in solution were performed in a semi-micro fluorescence cell (Hellma®, 104F-QS, 10 × 4 mm, 1400 μL) with a Varian Cary Eclipse spectrophotometer. Mass spectra were obtained on a Nippon Denshi JMS-01SG-2 mass spectrometer at an ionization energy of 70 eV using a direct inlet system through GLC. Elemental analyses were performed by a Yanaco MT-5.

*2.2. General procedure for synthesis of compound **1** and **2**.*

Insert Scheme 1 in here

A solution of 1-azidomethylpyrene (230 mg, 0.89 mmol) and copper iodide (10 mg) was added to **3** (185 mg, 0.27 mmol) or **4** (200 mg, 0.27 mmol) in THF/H_2O (v/v, 5:1, 30 mL), respectively, and the heterogeneous mixture was stirred at 70 °C for 24 h. The resulting solution was cooled and extracted twice with CH_2Cl_2. The organic extracts were combined, dried over $MgSO_4$, and then evaporated to give the solid

crude products. Column chromatography on silica gel eluting with 1:1 hexane/chloroform gave white solid compounds **1** and **2** in 63 % and 72 % yield, respectively.

Compound ***1.*** Mp. 139–141°C. ^{1}H NMR (400 MHz, $CDCl_3$): δ = 0.97 (s, 27H, *t*Bu), 4.21 (s, 6H, ArO–CH_2–triazole), 4.23–4.34 (AB q, 12H, ether bridge, J = 10.8 Hz), 5.75 (s, 6H, triazole–CH_2–pyrene), 6.78 (s, 6H, Ar*H*), 7.21 (s, 3H, triazole–*H*), 7.62–7.64 (d, 3H, pyrene–*H*, J = 7.6 Hz), 7.80–7.93 (m, 18H, pyrene–*H*), 7.99–8.00 (d, 3H, pyrene–*H*, J = 7.6 Hz), 8.07–8.10 (d, 3H, pyrene–*H*, J = 9.2 Hz). ^{13}C NMR (100 MHz, $CDCl_3$) δ = 31.4, 34.1, 51.7, 66.8, 69.5, 121.9, 123.4, 124.1, 124.5, 124.7, 125.4, 125.5, 125.9, 126.0, 127.0, 127.2, 127.3, 127.9, 128.6, 128.7, 130.2, 130.8, 130.9, 131.6, 144.2, 146.2, 152.1. MS: *m/z* 1462.68 (M^+). Anal. Calcd for $C_{96}H_{87}N_9O_{12}$ (1462.77): C 78.82, H 5.99, N 8.62. Found: C 78.99, H 6.14, N 8.47.

Compound ***2.*** Mp. 214–216 °C. ^{1}H NMR (400 MHz, $CDCl_3$): δ = 1.27–1.31 (t, 9H, $COOCH_2CH_3$, J = 6.8 Hz), 4.17–4.20 (d, 6H, ArCH_2*(eq)*O, J = 13.2 Hz), 4.19–4.24 (q, 6H, COOCH_2CH_3, J = 6.8 Hz), 4.31 (s, 6H, ArO–CH_2–triazole), 4.31–4.34 (d, 6H, ArCH_2*(ax)*O, J = 13.2 Hz), 5.78 (s, 6H, triazole–CH_2–pyrene), 7.29 (s, 3H, triazole–*H*), 7.39 (s, 6H, Ar*H*), 7.64–7.66 (d, 3H, pyrene–*H*, J = 8.0 Hz), 7.80–7.88 (m, 12H, pyrene–*H*), 7.90–7.94 (t, 6H, pyrene–*H*, J = 8.0 Hz), 7.98–8.00 (d, 3H, pyrene–*H*, J = 8.0 Hz), 8.02–8.04 (d, 3H, pyrene–*H*, J = 8.0 Hz). ^{13}C NMR (100 MHz, $CDCl_3$) δ = 14.3, 51.8, 60.6, 66.9, 68.9, 121.7, 123.4, 124.1, 124.6, 124.7, 125.5, 125.6, 126.1, 126.1, 126.9, 127.0, 127.3, 127.9, 128.6, 128.7, 130.2, 130.8, 131.1, 131.7, 131.8, 143.6, 158.2, 165.4. FABMS: *m/z* 1510.56 (M^+),

1511.57($M+H^+$). Anal. calcd for $C_{93}H_{75}N_9O_{12}$ (1510.64): C 73.94, H 5.00, N 8.34. found: C 73.89, H 5.04, N 8.36.

2.3 General procedure for the UV–vis and fluorescence titrations

For absorption or fluorescence measurements, compounds were dissolved in acetonitrile to obtain stock solutions (1 mM). The stock solutions were diluted with acetonitrile to the desired concentration. In titration experiments, typically, aliquots of freshly prepared standard solutions (10^{-3} M to 10^{-6} M) of various analytes in acetonitrile were added to record the UV–vis and fluorescence spectra.

3. Results and discussion

Sensors **1** and **2** were synthesized through click chemistry following our previous reports [35,36]. During this synthesis process, the Cu(I) was shown not only to catalyze the cycloaddition of alkynes and azides, but also produced a metal template effect. Thus, **1** and **2** were immobilized to the *cone* conformation. Sensors **1** and **2** exhibited almost identical spectral features (UV−vis and fluorescence). The UV−vis absorption spectra displayed absorption bands characteristic of pyrene with absorption maximum at 328 and 343 nm, while their emission spectra exhibited strong bands with excimer emission maximum at 484 nm upon excitation at 343 nm.

Insert Fig. 1 in here

To explore the potential application of compounds **1** and **2** as chemosensors for the detection of nitro-containing explosives, several analytes were used for fluorescence titration experiments. The fluorescence titration of **1** and **2** with TNP revealed that the

fluorescence emission intensity rapidly died down upon addition of increasing amounts of TNP (Fig. 1 and Fig. S1); the decrease in fluorescence emission could be readily observed under illumination at 365 nm (Fig. 1, insert). These results implied that there are strong interactions between the sensors and TNP, and that the quenching of fluorescence emission might occur due to the formation of a possible non-fluorescent complex. Based on the fluorescence titration results, the Stern–Volmer plot was found to be linear at lower concentrations (up to 100 μM, Fig. 2), which indicates that fluorescence quenching involves a static quenching mechanism at lower concentrations of TNP. The Stern–Volmer constants were calculated to be $K_{sv} = 2.23 \times 10^4\ M^{-1}$ (**1**) and $K_{sv} = 1.04 \times 10^4\ M^{-1}$ (**2**), respectively. In particular, at higher concentrations, the plot was found to be a hyperbolic curve (Fig. S2), which may be attributed to a combination of both static and dynamic (collision) quenching [37-39].

Insert Fig. 2 in here

The relative fluorescence quenching efficiencies of various analytes towards sensors **1** and **2** are summarized in the bar diagram (Fig. 3). The quenching efficiency was high for the electron deficient nitroaromatic compounds having an acidic -OH group. The order of the quenching efficiency was found to be TNP > NP, which is in complete agreement with the order of acidity of these analytes (TNP > NP). This may explain the unprecedented selectivity for TNP, as other nitro-compounds do not have a hydroxyl group and so they cannot interact strongly with the chemosensor and so result in a very low quenching effect. TNP, with its highly acidic hydroxyl group,

interacts strongly with the chemosensor and results in very high fluorescence quenching. These results demonstrate that both chemosensors **1** and **2** have high selectivity for TNP compared to other nitro-compounds. Importantly, the detection limit for TNP lies in the ppb range (70 ppb for sensor **1**) (Fig. S3 and S4) and the response time is very fast (seconds). Moreover, the extent of emission quenching of **1** in the presence of 100 equiv. of TNP after 10 seconds was practically identical to that after 2 hours (Fig. S5). These experimental results demonstrate that compounds **1** and **2** can be used as fluorescent sensor for TNP detection. Furthermore, **1** and **2** behave as better TNP sensor compared with many previous sensors reported in terms of selectivity, sensitivity and detection limit (Table S1). This analyte-induced reduction in emission intensity is ascribed to the formation of charge-transfer complexes between the electron donor (chemosensor) and the electron acceptor (analyte) [40]. Such a mechanistic rationale is consistent with previous reports in which it was suggested that thermodynamically favourable exciplex formation between a fluorophore and a quencher involves strong coupling of the respective π electrons, which in turn leads to deactivation of the fluorophore excited singlet state [41].

Insert Fig. 3 in here

The high sensitivity of sensor **1** towards TNP and the non-linear nature of the Stern–Volmer plot for TNP suggested that an energy transfer process might also be involved in the quenching process. As a matter of fact, when the absorption band of the non-emissive analyte display overlaps with the emission spectra of the fluorophore,

resonance energy transfer can effectively occur [42,43]. As shown in Fig. 4, a distinct spectral overlap of the absorption spectrum of TNP and the emission spectrum of sensor **1** over the range 375–475 nm was observed. In particular, there is a larger spectral overlap when TNP exists as picrate in the presence of the amine. Resonance energy transfer from sensor to picrate could make an additional contribution to the fluorescence quenching process [44,45]. Therefore, in solution both charge-transfer and resonance energy transfer contributed to the amplified quenching of fluorescence of the present systems.

Insert Fig. 4 in here

Insert Fig. 5 in here

Efforts were also made to determine whether sensor **1** could be used as a naked-eye detectable colorimetric chemosensor for TNP. As shown in Fig.5 (insert), on addition of TNP to solutions of **1**, a remarkable and easily visible color change was observed from pale yellow to reddish orange, which indicated the formation of the **1**•TNP complex. This color change is characterized by corresponding changes in the UV-Vis absorption spectrum. UV-Vis absorption titrations of **1** and **2** with TNP showed a steady increase in the peak intensity on increasing the concentration of TNP (Fig. 5 and Fig. S6). It thus provides further support for the proposed charge-transfer interaction between the electron-rich receptor and the electron deficient analyte and is consistent with the proposed charge-transfer based fluorescence quenching. According to the titration results, a linear relationship between the absorption intensity (at 343

nm) and concentration of TNP was observed (Fig. S7 and Fig. S8), which indicates that chemosensor **1** and **2** can be used for colorimetric detection of TNP.

Insert Fig. 6 in here

In order to employ the detection in a feasible method, a test strip was conveniently prepared by dip coating a solution of **1** onto a filter paper and then subsequently drying in air. As shown in Fig. 6, with the increase of TNP, there was an obvious difference of quenching. When the concentration of TNP reached the 0.5 mM level, the fluorescence was completely quenched.

Insert Fig. 7 in here

Insert Fig. 8 in here

To explore the mechanism and to identify the actual binding position of TNP, ^{1}H NMR titrations involving TNP and sensors **1** and **2** were performed. As shown in Fig. 7, the signals of H_a, H_b and H_c were clearly shifted downfield upon the addition of 15 equiv. of TNP into the solution of sensor **1** ($\Delta\delta$ = 0.17, 0.47 and 0.14 ppm, respectively). In the case of sensor **2**, upon addition of 30 equiv. of TNP to the solution of **2**, the peaks for H_a, H_b and H_c exhibited a similar but smaller downfield shift by $\Delta\delta$ = 0.17, 0.33 and 0.13 ppm, respectively (Fig. S9). From the spectral shifts, it was observed that proton H_b underwent the maximum chemical shift, whereas protons H_a and H_c proximal to the triazole rings underwent a smaller chemical shift. These downfield shifts were ascribed to TNP withdrawing electron density from the sensor. The significant change in the chemical shift of proton H_b suggested that the C–H bond of the triazole group acts as the receptor site. It is

possible that CH···O hydrogen bonding between H_b and TNP was formed, thus a plausible binding mode between **1** and TNP is presented (Fig. 8). Hence, these results clearly indicate that intermolecular charge transfer takes place between the sensor and TNP. Based on the differences in the induced fluorescence quenching response, greater changes in the chemical shift for sensor **1** were seen upon the addition of TNP than for sensor **2** (for the same number of molar equivalents). It suggests that sensor **1** is more effective and sensitive for the detection of TNP in comparison to sensor **2**.

4. Conclusions

In summary, we have designed and synthesized two click-modified hexahomotrioxacalix[3]arenes **1** and **2**, each of which can be utilized as fluorometric and colorimetric chemosensor for 2,4,6-trinitrophenol. Chemosensor **1** and **2** exhibited high binding affinity and selectivity toward 2,4,6-trinitrophenol as evidenced by UV-vis and fluorescence studies. ^{1}H NMR spectroscopic titrations revealed **1**•TNP complex formed via CH···O hydrogen bonding interaction. As a general design strategy, structural modifications by click chemistry may allow us to develop further chemosensor candidates for the future detection of nitro-containing explosives.

Acknowledgments

This work was performed under the Cooperative Research Program of "Network Joint Research Center for Materials and Devices (Institute for Materials Chemistry and Engineering, Kyushu University)". We thank the

OTEC at Saga University and the International Cooperation Projects of Guizhou Province (No. 20137002). The EPSRC is thanked for an overseas travel grant to CR.

Appendix A. Supplementary data

References

[1] X. Zhou, S. Lee, Z. Xu, J. Yoon, Recent progress on the development of chemosensors for gases, Chem. Rev. 115 (2015) 7944–8000.

[2] Y. Zhou, J. Yoon, Recent progress in fluorescent and colorimetric chemosensors for detection of amino acids, Chem. Soc. Rev. 41 (2012) 52–67.

[3] J.F. Zhang, Y. Zhou, J. Yoon, J.S. Kim, Recent progress in fluorescent and colorimetric chemosensors for detection of precious metal ions (silver, gold and platinum ions), Chem. Soc. Rev. 40 (2011) 3416–3429.

[4] J. Wu, W. Liu, J. Ge, H. Zhang, P. Wang, New sensing mechanisms for design of fluorescent chemosensors emerging in recent years, Chem. Soc. Rev. 40 (2011) 3483–3495.

[5] F. Akhgari, H. Fattahi, Y.M. Oskoei, Recent advances in nanomaterial-based sensors for detection of trace nitroaromatic explosives, Sens. Actuators B 221 (2015) 867–878.

[6] J.S. Caygill, F. Davis, S.P.J. Higson, Current trends in explosive detection techniques, Talanta 88 (2012) 14–29.

[7] E. Holmgren, S. Ek, A. Colmsjö, Extraction of explosives from soil followed by gas chromatography–mass spectrometry analysis with negative chemical ionization, J

Chromatogr. A 1222 (2012) 109–115.

[8] C. Cortada, L. Vidal, A. Canals, Determination of nitroaromatic explosives in water samples by direct ultrasound-assisted dispersive liquid–liquid microextraction followed by gas chromatography–mass spectrometry, Talanta 85 (2011) 2546–2552.

[9] S. Schramm, D. Vailhen, M.C. Bridoux, Use of experimental design in the investigation of stir bar sorptive extraction followed by ultra-high-performance liquid chromatography–tandem mass spectrometry for the analysis of explosives in water samples, J. Chromatogr. A 1433 (2016) 24–33.

[10] S. Babaee, A. Beiraghi, Micellar extraction and high performance liquid chromatography-ultra violet determination of some explosives in water samples, Anal. Chim. Acta 662 (2010) 9–13.

[11] J. Lee, S. Park, S.G. Cho, E.M. Goh, S. Lee, S.-S. Koh, J. Kim, Analysis of explosives using corona discharge ionization combined with ion mobility spectrometry–mass spectrometry, Talanta 120 (2014) 64–70.

[12] M. Tabrizchi, V. ILbeigi, Detection of explosives by positive corona discharge ion mobility spectrometry, J. Hazard. Mater. 176 (2010) 692–696.

[13] K.L. Gares, K.T. Hufziger, S.V. Bykov, S.A. Asher, Review of explosive detection methodologies and the emergence of standoff deep UV resonance Raman, J. Raman Spectrosc. 47 (2016) 124–141.

[14] A. Hakonen, P.O. Andersson, M.S. Schmidt, T. Rindzevicius, M. Käll, Explosive and chemical threat detection by surface-enhanced Raman scattering: A review, Anal. Chim. Acta 893 (2015) 1–13.

[15] J. Riedel, M. Berthold, U. Guth, Electrochemical determination of dissolved nitrogen-containing explosives, Electrochimica Acta 128 (2014) 85–90.

[16] J. Zang, C.X. Guo, F. Hu, L. Yu, C.M. Li, Electrochemical detection of ultratrace nitroaromatic explosives using ordered mesoporous carbon, Anal. Chim. Acta 683 (2011) 187–191.

[17] M.S. Meaney, V.L. McGuffin, Investigation of common fluorophores for the detection of nitrated explosives by fluorescence quenching, Anal. Chim. Acta 610 (2008) 57–67.

[18] R. Tu, B. Liu, Z. Wang, D. Gao, F. Wang, Q. Fang, Z. Zhang, Amine-capped ZnS−Mn^{2+} nanocrystals for fluorescence detection of trace TNT, Anal. Chem. 80 (2008) 3458–3465.

[19] M.E. Germain, M.J. Knapp, Optical explosives detection: from color changes to fluorescence turn-on, Chem. Soc. Rev. 38 (2009) 2543–2555.

[20] X. Sun, Y. Wang, Y. Lei, Fluorescence based explosive detection: from mechanisms to sensory materials, Chem. Soc. Rev. 44 (2015) 8019–8061.

[21] R.L. Woodfin, Trace chemical sensing of explosives, John Wiley & Sons, Inc., Hoboken, NJ, USA, 2006, pp. 193–209 (Chapter 9).

[22] S.J. Toal, W.C. Trogler, Polymer sensors for nitroaromatic explosives detection, J. Mater. Chem. 16 (2006) 2871–2883.

[23] Z. Hu, B.J. Deibert, J. Li, Luminescent metal–organic frameworks for chemical sensing and explosive detection, Chem. Soc. Rev. 43 (2014) 5815–5840.

[24] S. Shanmugaraju, P.S. Mukherjee, π-Electron rich small molecule sensors for the

recognition of nitroaromatics, Chem. Commun. 51 (2015) 16014–16032.

[25] Y. Salinas, R. Martínez-Máñez, M.D. Marcos, F. Sancenón, A.M. Costero, M. Parra, S. Gil, Optical chemosensors and reagents to detect explosives, Chem. Soc. Rev. 41 (2012) 1261–1296.

[26] R. Joseph, C.P. Rao, Ion and molecular recognition by lower rim 1,3-di-conjugates of calix[4]arene as receptors, Chem. Rev. 111 (2011) 4658–4702.

[27] J.S. Kim, D.T. Quang, Calixarene-derived fluorescent probes, Chem. Rev. 107 (2007) 3780−3799.

[28] H.C. Kolb, M.G. Finn, K.B. Sharpless, Click chemistry: diverse chemical function from a few good reactions, Angew. Chem. Int. Ed. 40 (2001) 2004–2021.

[29] J.J. Bryant, U.H.F. Bunz, Click to bind: metal sensors, Chem. Asian J. 8 (2013) 1354–1367.

[30] Y.H. Lau, P.J. Rutledge, M. Watkinson, M.H. Todd, Chemical sensors that incorporate click-derived triazoles, Chem. Soc. Rev. 40 (2011) 2848–2866.

[31] M. Song, Z. Sun, C. Han, D. Tian, H. Li, J.S. Kim, Calixarene-based chemosensors by means of click chemistry, Chem. Asian J. 9 (2014) 2344–2357.

[32] D. Schweinfurth, S. Strobel, B. Sarkar, Expanding the scope of 'Click' derived 1,2,3-triazole ligands: New palladium and platinum complexes, Inorg. Chim. Acta 374 (2011) 253–260.

[33] D. Urankar, A. Pevec, I. Turel, J. Košmrlj, Pyridyl conjugated 1,2,3-triazole is a versatile coordination ability ligand enabling supramolecular associations, Cryst. Growth Des. 10 (2010) 4920–4927.

[34] B. Gole, S. Shanmugaraju, A.K. Bara, P.S. Mukherjee, Supramolecular polymer for explosives sensing: role of H-bonding in enhancement of sensitivity in the solid state, Chem. Commun. 47 (2011) 10046–10048.

[35] X.L. Ni, S. Wang, X. Zeng, Z. Tao, T. Yamato, Pyrene-linked triazole-modified homooxacalix[3]arene: a unique C_3 symmetry ratiometric fluorescent chemosensor for Pb^{2+}, Org. Lett. 13 (2011) 552–555.

[36] C. Wu, Y. Ikejiri, J.L. Zhao, X.K. Jiang, X.L. Ni, X. Zeng, C. Redshaw, T. Yamato, A pyrene-functionalized triazole-linked hexahomotrioxacalix[3]arene as a fluorescent chemosensor for Zn^{2+} ions, Sens. Actuators B 228 (2016) 480–485.

[37] M.K. Chahal, M. Sankar, 1,8-Naphthyridine-based fluorescent receptors for picric acid detection in aqueous media, Anal. Methods 7 (2015) 10272–10279.

[38] S.S. Nagarkar, A.V. Desai, S.K. Ghosh, A fluorescent metal–organic framework for highly selective detection of nitro explosives in the aqueous phase, Chem. Commun. 50 (2014) 8915–8918.

[39] V. Bhalla, H. Arora, H. Singh, M. Kumar, Triphenylene derivatives: chemosensors for sensitive detection of nitroaromatic explosives, Dalton Trans. 42 (2013) 969–974.

[40] S. Shanmugaraju, P.S. Mukherjee, Self-assembled discrete molecules for sensing nitroaromatics, Chem. Eur. J. 21 (2015) 6656–6666.

[41] Y.H. Lee, H. Liu, J.Y. Lee, S.H. Kim, S.K. Kim, J.L. Sessler, Y. Kim, J.S. Kim, Dipyrenylcalix[4]arene–a fluorescence-based chemosensor for trinitroaromatic explosives, Chem. Eur. J. 16 (2010) 5895–5901.

[42] B. Joarder, A.V. Desai, P. Samanta, S. Mukherjee, S.K. Ghosh, Selective and sensitive aqueous-phase detection of 2,4,6-trinitrophenol (TNP) by an amine-functionalized metal–organic framework, Chem. Eur. J. 21 (2015) 965–969.

[43] S.S. Nagarkar, B. Joarder, A.K. Chaudhari, S. Mukherjee, S.K. Ghosh, Highly selective detection of nitro explosives by a luminescent metal–organic framework, Angew. Chem. Int. Ed. 52 (2013) 2881–2885.

[44] R. Chopra, P. Kaur, K. Singh, Pyrene-based chemosensor detects picric acid upto attogram level through aggregation enhanced excimer emission, Anal. Chim. Acta 864 (2015) 55–63.

[45] S. Hussain, A.H. Malik, M.A. Afroz, P.K. Iyer, Ultrasensitive detection of nitroexplosive – picric acid via a conjugated polyelectrolyte in aqueous media and solid support, Chem. Commun. 51 (2015) 7207–7210.

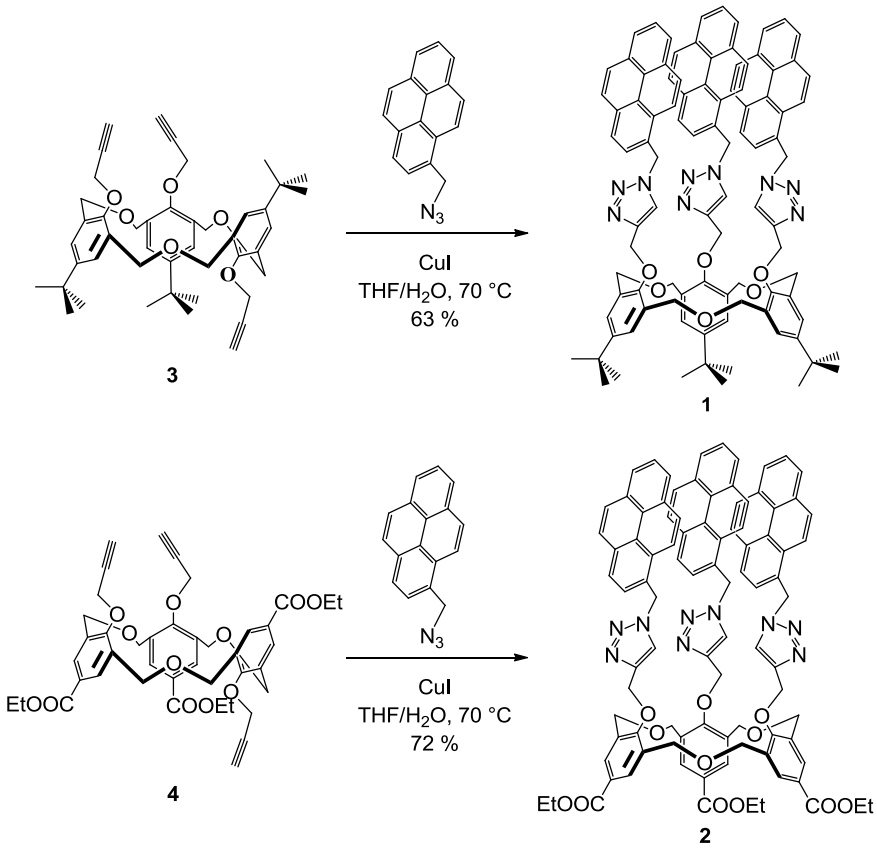

Scheme 1 The synthetic route of chemosensors **1** and **2**.

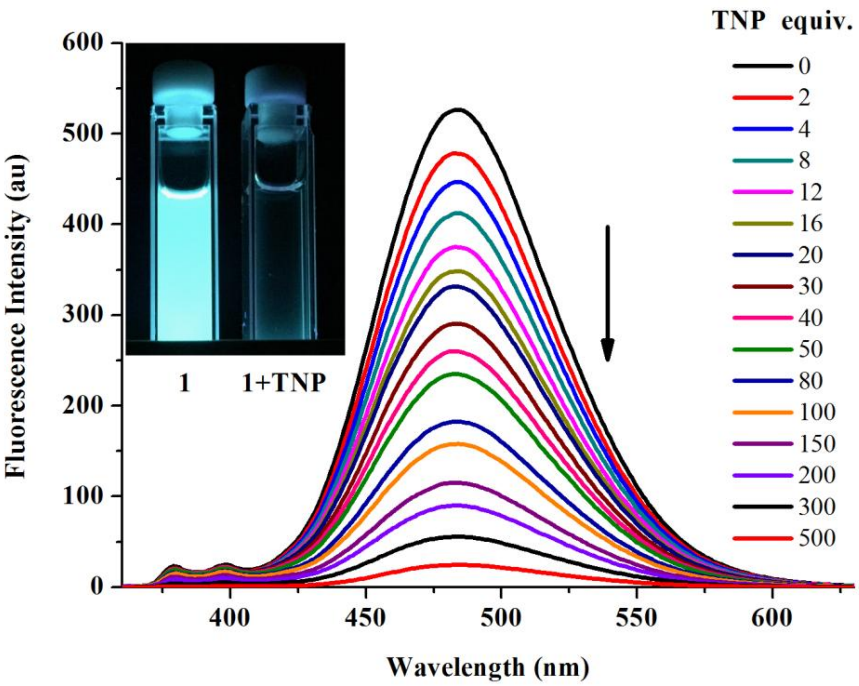

Fig. 1 Fluorescence emission spectra of **1** (1.0 μM) upon the addition of increasing concentrations of TNP in CH_3CN. λ_{ex} = 343 nm. The inset shows the fluorescence color of **1** before and after the addition of TNP.

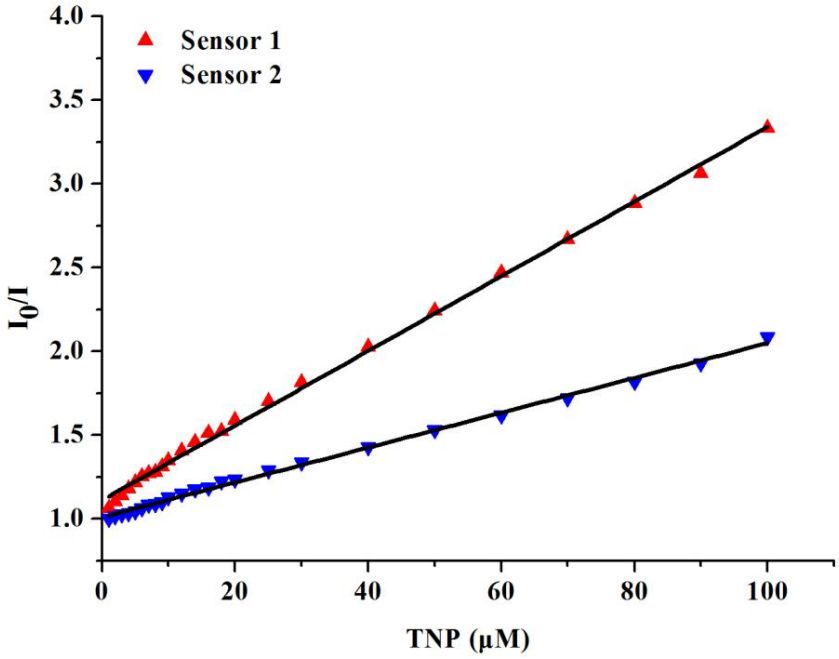

Fig. 2 Stern–Volmer plots for the titration of sensors **1** and **2** with TNP at lower concentrations (up to 100 μM).

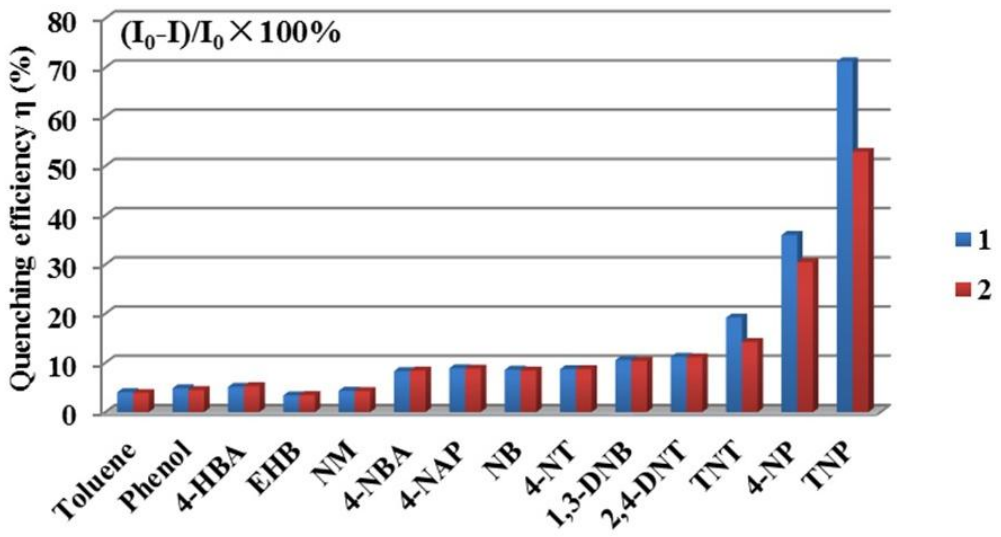

Fig. 3 Reduction in fluorescence intensity (plotted as quenching efficiency) seen upon the addition of 100 equiv. of analytes. 4-HBA = 4-hydroxybenzoic acid, EHB = ethyl 4-hydroxybenzoate, NM = nitromethane, 4-NBA = 4-nitrobenzoic acid, 4-NAP = 4-nitroacetophenone, NB = nitrobenzene, 4-NT = 4-nitrotoluene, 1,3-DNB = 1,3-dinitrobenzene, 2,4-DNT = 2,4-dinitrotoluene, TNT = 2,4,6-trinitrotoluene, 4-NP = 4-nitrophenol and TNP = 2,4,6-trinitrophenol.

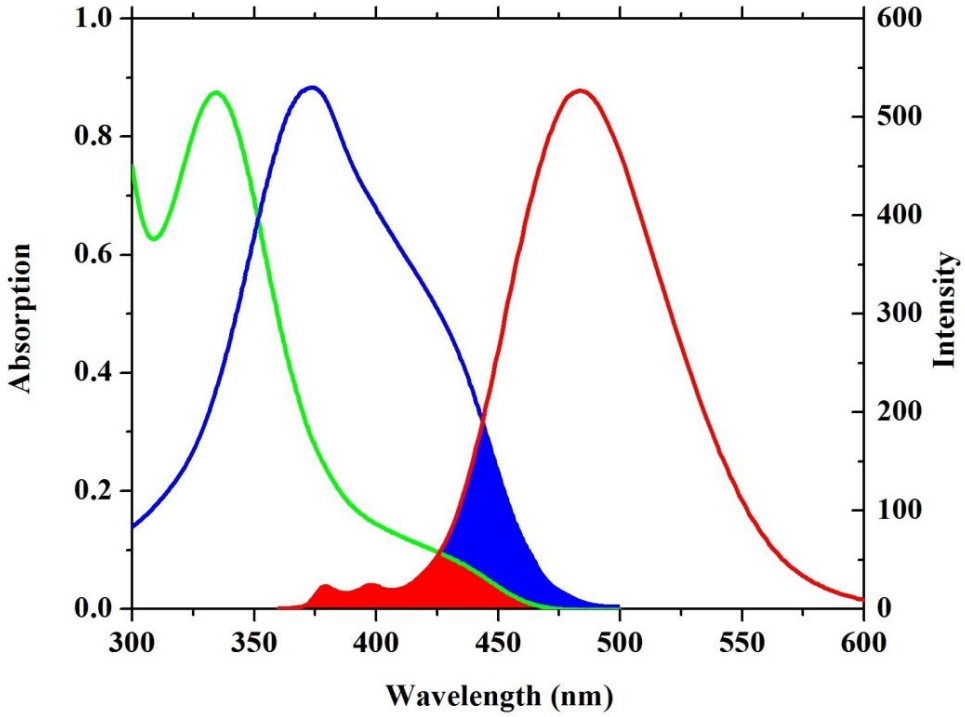

Fig. 4 Spectral overlaps between absorption spectra of TNP (green line), TNP in the presence of amine (blue line) and the emission spectrum of **1** (red line).

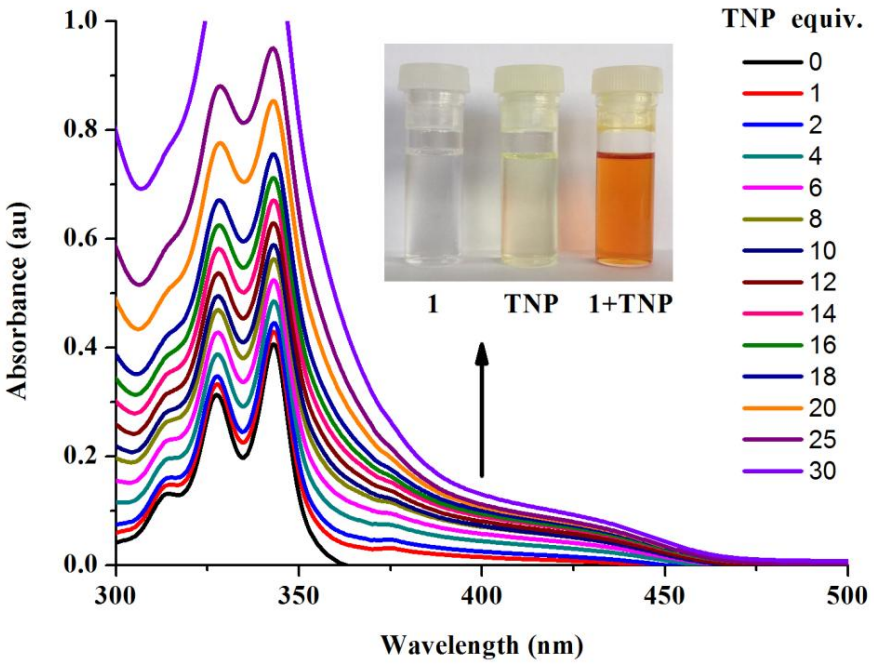

Fig. 5 Change in absorption spectra of sensor **1** (5.0 μM) with the addition of TNP in CH_3CN. Inset: visual colour change due to the formation **1**•TNP complex.

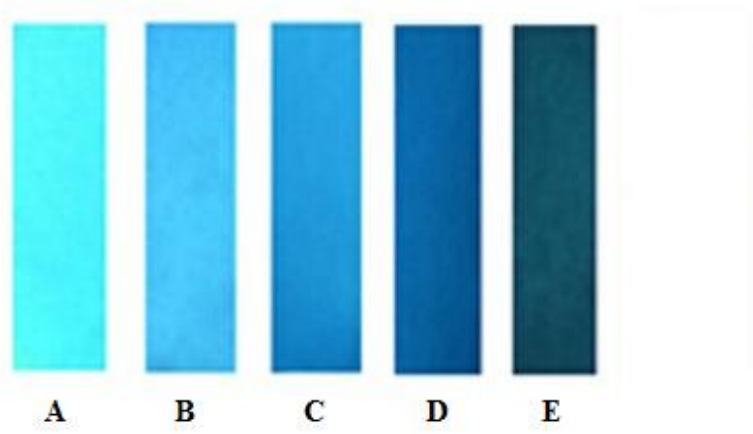

Fig. 6 Photographs (under 365 nm UV light) of the fluorescence response of **1** on test strips after contact with various concentrations of TNP: (A) 0.0 μM, (B) 5.0 μM, (C) 10.0 μM, (D) 100.0 μM and (E) 0.5 mM.

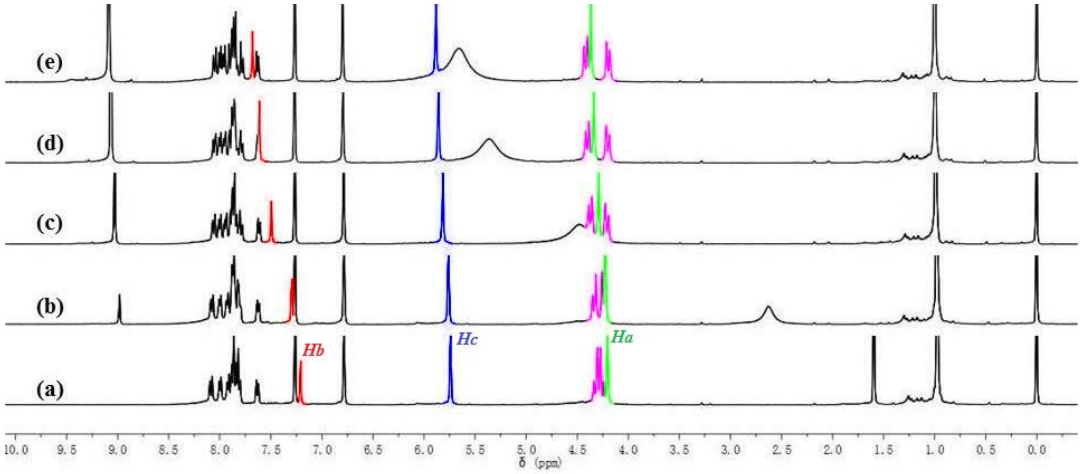

Fig. 7 The ^{1}H NMR spectra of **1** (5.0 mM) upon titration with TNP in $CDCl_3$. (a) **1** only, (b c d and e) in the presence of 1.0, 5.0, 10.0 and 15.0 equiv. of TNP, respectively.

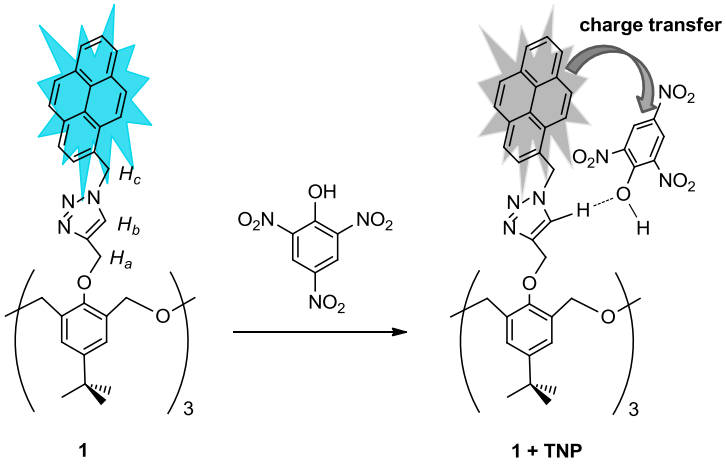

Fig. 8 Plausible binding mode between **1** and TNP.

Electronic Supplementary Material (online publication only)

Click here to download Electronic Supplementary Material (online publication only): 6. 0620 SI R1.pdf

Click-modified hexahomotrioxacalix[3]arenes as fluorometric and colorimetric dual-modal chemosensor for 2,4,6-trinitrophenol

Chong Wu,[a] Jiang-Lin Zhao,[a] Xue-Kai Jiang,[a] Xin-Long Ni,[b] Xi Zeng,[b] Carl Redshaw[c] and Takehiko Yamato*[a]

[a] Department of Applied Chemistry, Faculty of Science and Engineering, Saga University, Honjo-machi 1, Saga 840-8502, Japan

[b] Key Laboratory of Macrocyclic and Supramolecular Chemistry of Guizhou Province, Guizhou University, Guiyang 550025, People's Republic of China

[c] Department of Chemistry, The University of Hull, Cottingham Road, Hull, Yorkshire, HU6 7RX, UK

ABSTRACT: A new type of chemosensor-based approach to the detection of 2,4,6-trinitrophenol (TNP) is described in this paper. Two hexahomotrioxacalix[3]arene-based chemosensors **1** and **2** were synthesized through click chemistry, which exhibited high binding affinity and selectivity toward TNP as evidenced by UV-vis and fluorescence spectroscopy studies. ^{1}H NMR titration analysis verified that CH···O hydrogen bonding is demonstrated as the mode of interaction, which possibly facilitates effective charge-transfer.

Keywords: Hexahomotrioxacalix[3]arene, Click chemistry, Colorimetric chemosensor, Fluorometric chemosensor, 2,4,6-Trinitrophenol.

* Corresponding author. Fax: +81 952 28 8548.
E-mail address: yamatot@cc.saga-u.ac.jp (T. Yamato).

Graphical Abstract

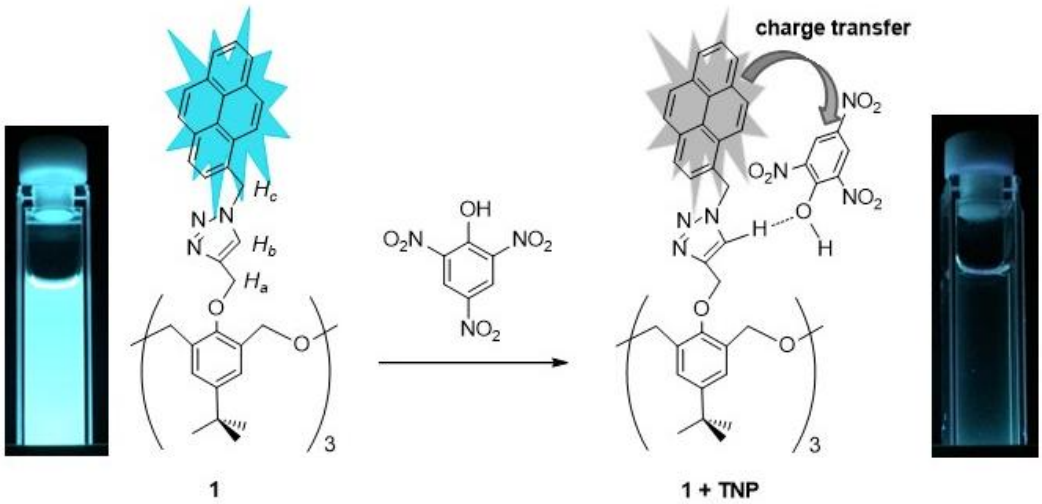

Highlight:

➢Click-modified hexahomotrioxacalix[3]arene is developed for the first time to detection TNP.

➢Fluorometric and colorimetric dual-modal chemosensor for TNP.

➢Highly selective and sensitive are obtained and the detection limit is 70 ppb.

➢A novel design strategy for developing chemosensors for TNP has been demonstrated.

1. Introduction

The design of chemosensors that are able to selectively recognize and sense specific analytes is an attractive research area in supramolecular chemistry [1-4]. In particular, the rapid and accurate detection of nitro-containing explosives is a high priority for security and health/environmental issues [5-6]. Various analytical techniques such as gas chromatography coupled with different detectors [7,8], high performance liquid chromatography [9,10], ion-mobility spectroscopy [11,12], Raman or surface enhanced Raman spectroscopy [13,14], electrochemical methods [15,16] and fluorescence spectroscopy [17,18] have been used for the detection of nitro-containing explosives. Among these techniques, fluorescence-based detection offers several advantages over other analytical methods with respect to high sensitivity, specificity, and real-time monitoring with fast response times [19]. To date, considerable effort has been devoted to the development of fluorescence sensing materials to detect nitro-containing explosives [20,21]. Even though several π-conjugated polymers [22] and metal-organic frameworks [23] have been employed to detect nitro-containing explosives, the development of reliable and efficient organic chemosensors possessing high selectivity for nitro-containing explosives remains a very challenging task [24,25].

Calixarenes are ideal frameworks for the development of chemosensors in the molecular recognition of chemical and biological targets of interest since the incorporation of a suitable sensory group into the calixarene results in a tailored

chromogenic receptor [26,27]. In particular, since Sharpless et al. developed click chemistry as a new coupling strategy in 2001 [28], numerous calixarene derivatives incorporating click-derived triazoles have been reported, which can be used as metal ions chemosensors via coordination at nitrogen atom [29-31]. However, these fluorescence systems have scarcely been exploited for the sensing of nitro-containing explosives. As a matter of fact, given the strong dipolar character of the triazole ring, the C–H bond of the heterocycle makes a surprisingly good hydrogen bond donor [32,33]. On the other hand, nitro-containing explosives often act as good electron acceptors due to the presence of electron withdrawing nitro ($-NO_2$) group/s [34]. Considering these two opposite properties of triazole and nitro-containing explosives, one might consider if noncovalent interactions exist between them?

In molecular recognition processes, noncovalent interactions such as hydrogen bonding, aromatic π-stacking and weak intermolecular interactions play a crucial role. With this in mind, can we utilize the click-derived triazole to design chemosensors for nitro-containing explosive sensing? Herein, we report two triazole-modified hexahomotrioxacalix[3]arenes **1** and **2** as a new type of chemosensor for the selective detection of 2,4,6-trinitrophenol (TNP) explosive. To the best of our knowledge, this is the first report where a triazole-modified hexahomotrioxacalix[3]arene serves as a selective chemosensor for TNP.

2. Experimental section

2.1. General

Unless otherwise stated, all reagents were purchased from commercial sources and used without further purification. All solvents were dried and distilled by the usual procedures before use. Melting points were determined using a Yanagimoto MP-S1. ^{1}H NMR and ^{13}C NMR spectra were recorded on a Nippon Denshi JEOL FT-300 NMR spectrometer and a Varian-400MRvnmrs400 with $SiMe_4$ as an internal reference: *J*-values are given in Hz. IR spectra were measured as KBr pellets or as liquid films on NaCl plates in a Nippon Denshi JIR-AQ2OM spectrophotometer. UV spectra were measured by a Shimadzu UV-3150UV-vis-NIR spectrophotometer. Fluorescence spectroscopic studies of compounds in solution were performed in a semi-micro fluorescence cell (Hellma®, 104F-QS, 10 × 4 mm, 1400 μL) with a Varian Cary Eclipse spectrophotometer. Mass spectra were obtained on a Nippon Denshi JMS-01SG-2 mass spectrometer at an ionization energy of 70 eV using a direct inlet system through GLC. Elemental analyses were performed by a Yanaco MT-5.

*2.2. General procedure for synthesis of compound **1** and **2**.*

Insert Scheme 1 in here

A solution of 1-azidomethylpyrene (230 mg, 0.89 mmol) and copper iodide (10 mg) was added to **3** (185 mg, 0.27 mmol) or **4** (200 mg, 0.27 mmol) in THF/H_2O (v/v, 5:1, 30 mL), respectively, and the heterogeneous mixture was stirred at 70 °C for 24 h. The resulting solution was cooled and extracted twice with CH_2Cl_2. The organic extracts were combined, dried over $MgSO_4$, and then evaporated to give the solid

crude products. Column chromatography on silica gel eluting with 1:1 hexane/chloroform gave white solid compounds **1** and **2** in 63 % and 72 % yield, respectively.

*Compound **1**.* Mp. 139–141°C. ^{1}H NMR (400 MHz, $CDCl_3$): δ = 0.97 (s, 27H, *t*Bu), 4.21 (s, 6H, ArO–CH_2–triazole), 4.23–4.34 (AB q, 12H, ether bridge, J = 10.8 Hz), 5.75 (s, 6H, triazole–CH_2–pyrene), 6.78 (s, 6H, Ar*H*), 7.21 (s, 3H, triazole–*H*), 7.62–7.64 (d, 3H, pyrene–*H*, J = 7.6 Hz), 7.80–7.93 (m, 18H, pyrene–*H*), 7.99–8.00 (d, 3H, pyrene–*H*, J = 7.6 Hz), 8.07–8.10 (d, 3H, pyrene–*H*, J = 9.2 Hz). ^{13}C NMR (100 MHz, $CDCl_3$) δ = 31.4, 34.1, 51.7, 66.8, 69.5, 121.9, 123.4, 124.1, 124.5, 124.7, 125.4, 125.5, 125.9, 126.0, 127.0, 127.2, 127.3, 127.9, 128.6, 128.7, 130.2, 130.8, 130.9, 131.6, 144.2, 146.2, 152.1. MS: *m/z* 1462.68 (M^+). Anal. Calcd for $C_{96}H_{87}N_9O_{12}$ (1462.77): C 78.82, H 5.99, N 8.62. Found: C 78.99, H 6.14, N 8.47.

*Compound **2**.* Mp. 214–216 °C. ^{1}H NMR (400 MHz, $CDCl_3$): δ = 1.27–1.31 (t, 9H, $COOCH_2CH_3$, J = 6.8 Hz), 4.17–4.20 (d, 6H, ArCH_2*(eq)*O, J = 13.2 Hz), 4.19–4.24 (q, 6H, COOCH_2CH_3, J = 6.8 Hz), 4.31 (s, 6H, ArO–CH_2–triazole), 4.31–4.34 (d, 6H, ArCH_2*(ax)*O, J = 13.2 Hz), 5.78 (s, 6H, triazole–CH_2–pyrene), 7.29 (s, 3H, triazole–*H*), 7.39 (s, 6H, Ar*H*), 7.64–7.66 (d, 3H, pyrene–*H*, J = 8.0 Hz), 7.80–7.88 (m, 12H, pyrene–*H*), 7.90–7.94 (t, 6H, pyrene–*H*, J = 8.0 Hz), 7.98–8.00 (d, 3H, pyrene–*H*, J = 8.0 Hz), 8.02–8.04 (d, 3H, pyrene–*H*, J = 8.0 Hz). ^{13}C NMR (100 MHz, $CDCl_3$) δ = 14.3, 51.8, 60.6, 66.9, 68.9, 121.7, 123.4, 124.1, 124.6, 124.7, 125.5, 125.6, 126.1, 126.1, 126.9, 127.0, 127.3, 127.9, 128.6, 128.7, 130.2, 130.8, 131.1, 131.7, 131.8, 143.6, 158.2, 165.4. FABMS: *m/z* 1510.56 (M^+),

1511.57($M+H^+$). Anal. calcd for $C_{93}H_{75}N_9O_{12}$ (1510.64): C 73.94, H 5.00, N 8.34. found: C 73.89, H 5.04, N 8.36.

2.3 General procedure for the UV–vis and fluorescence titrations

For absorption or fluorescence measurements, compounds were dissolved in acetonitrile to obtain stock solutions (1 mM). The stock solutions were diluted with acetonitrile to the desired concentration. In titration experiments, typically, aliquots of freshly prepared standard solutions (10^{-3} M to 10^{-6} M) of various analytes in acetonitrile were added to record the UV–vis and fluorescence spectra.

3. Results and discussion

Sensors **1** and **2** were synthesized through click chemistry following our previous reports [35,36]. During this synthesis process, the Cu(I) was shown not only to catalyze the cycloaddition of alkynes and azides, but also produced a metal template effect. Thus, **1** and **2** were immobilized to the *cone* conformation. Sensors **1** and **2** exhibited almost identical spectral features (UV−vis and fluorescence). The UV−vis absorption spectra displayed absorption bands characteristic of pyrene with absorption maximum at 328 and 343 nm, while their emission spectra exhibited strong bands with excimer emission maximum at 484 nm upon excitation at 343 nm.

Insert Fig. 1 in here

To explore the potential application of compounds **1** and **2** as chemosensors for the detection of nitro-containing explosives, several analytes were used for fluorescence titration experiments. The fluorescence titration of **1** and **2** with TNP revealed that the

fluorescence emission intensity rapidly died down upon addition of increasing amounts of TNP (Fig. 1 and Fig. S1); the decrease in fluorescence emission could be readily observed under illumination at 365 nm (Fig. 1, insert). These results implied that there are strong interactions between the sensors and TNP, and that the quenching of fluorescence emission might occur due to the formation of a possible non-fluorescent complex. Based on the fluorescence titration results, the Stern–Volmer plot was found to be linear at lower concentrations (up to 100 μM, Fig. 2), which indicates that fluorescence quenching involves a static quenching mechanism at lower concentrations of TNP. The Stern–Volmer constants were calculated to be $K_{sv} = 2.23 \times 10^4\ M^{-1}$ (**1**) and $K_{sv} = 1.04 \times 10^4\ M^{-1}$ (**2**), respectively. In particular, at higher concentrations, the plot was found to be a hyperbolic curve (Fig. S2), which may be attributed to a combination of both static and dynamic (collision) quenching [37-39].

Insert Fig. 2 in here

The relative fluorescence quenching efficiencies of various analytes towards sensors **1** and **2** are summarized in the bar diagram (Fig. 3). The quenching efficiency was high for the electron deficient nitroaromatic compounds having an acidic -OH group. The order of the quenching efficiency was found to be TNP > NP, which is in complete agreement with the order of acidity of these analytes (TNP > NP). This may explain the unprecedented selectivity for TNP, as other nitro-compounds do not have a hydroxyl group and so they cannot interact strongly with the chemosensor and so result in a very low quenching effect. TNP, with its highly acidic hydroxyl group,

interacts strongly with the chemosensor and results in very high fluorescence quenching. These results demonstrate that both chemosensors **1** and **2** have high selectivity for TNP compared to other nitro-compounds. Importantly, the detection limit for TNP lies in the ppb range (70 ppb for sensor **1**) (Fig. S3 and S4) and the response time is very fast (seconds). Moreover, the extent of emission quenching of **1** in the presence of 100 equiv. of TNP after 10 seconds was practically identical to that after 2 hours (Fig. S5). These experimental results demonstrate that compounds **1** and **2** can be used as fluorescent sensor for TNP detection. Furthermore, **1** and **2** behave as better TNP sensor compared with many previous sensors reported in terms of selectivity, sensitivity and detection limit (Table S1). This analyte-induced reduction in emission intensity is ascribed to the formation of charge-transfer complexes between the electron donor (chemosensor) and the electron acceptor (analyte) [40]. Such a mechanistic rationale is consistent with previous reports in which it was suggested that thermodynamically favourable exciplex formation between a fluorophore and a quencher involves strong coupling of the respective π electrons, which in turn leads to deactivation of the fluorophore excited singlet state [41].

Insert Fig. 3 in here

The high sensitivity of sensor **1** towards TNP and the non-linear nature of the Stern–Volmer plot for TNP suggested that an energy transfer process might also be involved in the quenching process. As a matter of fact, when the absorption band of the non-emissive analyte display overlaps with the emission spectra of the fluorophore,

resonance energy transfer can effectively occur [42,43]. As shown in Fig. 4, a distinct spectral overlap of the absorption spectrum of TNP and the emission spectrum of sensor **1** over the range 375–475 nm was observed. In particular, there is a larger spectral overlap when TNP exists as picrate in the presence of the amine. Resonance energy transfer from sensor to picrate could make an additional contribution to the fluorescence quenching process [44,45]. Therefore, in solution both charge-transfer and resonance energy transfer contributed to the amplified quenching of fluorescence of the present systems.

Insert Fig. 4 in here

Insert Fig. 5 in here

Efforts were also made to determine whether sensor **1** could be used as a naked-eye detectable colorimetric chemosensor for TNP. As shown in Fig.5 (insert), on addition of TNP to solutions of **1**, a remarkable and easily visible color change was observed from pale yellow to reddish orange, which indicated the formation of the **1**•TNP complex. This color change is characterized by corresponding changes in the UV-Vis absorption spectrum. UV-Vis absorption titrations of **1** and **2** with TNP showed a steady increase in the peak intensity on increasing the concentration of TNP (Fig. 5 and Fig. S6). It thus provides further support for the proposed charge-transfer interaction between the electron-rich receptor and the electron deficient analyte and is consistent with the proposed charge-transfer based fluorescence quenching. According to the titration results, a linear relationship between the absorption intensity (at 343

nm) and concentration of TNP was observed (Fig. S7 and Fig. S8), which indicates that chemosensor **1** and **2** can be used for colorimetric detection of TNP.

Insert Fig. 6 in here

In order to employ the detection in a feasible method, a test strip was conveniently prepared by dip coating a solution of **1** onto a filter paper and then subsequently drying in air. As shown in Fig. 6, with the increase of TNP, there was an obvious difference of quenching. When the concentration of TNP reached the 0.5 mM level, the fluorescence was completely quenched.

Insert Fig. 7 in here

Insert Fig. 8 in here

To explore the mechanism and to identify the actual binding position of TNP, ^{1}H NMR titrations involving TNP and sensors **1** and **2** were performed. As shown in Fig. 7, the signals of H_a, H_b and H_c were clearly shifted downfield upon the addition of 15 equiv. of TNP into the solution of sensor **1** ($\Delta\delta$ = 0.17, 0.47 and 0.14 ppm, respectively). In the case of sensor **2**, upon addition of 30 equiv. of TNP to the solution of **2**, the peaks for H_a, H_b and H_c exhibited a similar but smaller downfield shift by $\Delta\delta$ = 0.17, 0.33 and 0.13 ppm, respectively (Fig. S9). From the spectral shifts, it was observed that proton H_b underwent the maximum chemical shift, whereas protons H_a and H_c proximal to the triazole rings underwent a smaller chemical shift. These downfield shifts were ascribed to TNP withdrawing electron density from the sensor. The significant change in the chemical shift of proton H_b suggested that the C–H bond of the triazole group acts as the receptor site. It is

possible that CH···O hydrogen bonding between H_b and TNP was formed, thus a plausible binding mode between **1** and TNP is presented (Fig. 8). Hence, these results clearly indicate that intermolecular charge transfer takes place between the sensor and TNP. Based on the differences in the induced fluorescence quenching response, greater changes in the chemical shift for sensor **1** were seen upon the addition of TNP than for sensor **2** (for the same number of molar equivalents). It suggests that sensor **1** is more effective and sensitive for the detection of TNP in comparison to sensor **2**.

4. Conclusions

In summary, we have designed and synthesized two click-modified hexahomotrioxacalix[3]arenes **1** and **2**, each of which can be utilized as fluorometric and colorimetric chemosensor for 2,4,6-trinitrophenol. Chemosensor **1** and **2** exhibited high binding affinity and selectivity toward 2,4,6-trinitrophenol as evidenced by UV-vis and fluorescence studies. ^{1}H NMR spectroscopic titrations revealed **1**•TNP complex formed via CH···O hydrogen bonding interaction. As a general design strategy, structural modifications by click chemistry may allow us to develop further chemosensor candidates for the future detection of nitro-containing explosives.

Acknowledgments

This work was performed under the Cooperative Research Program of "Network Joint Research Center for Materials and Devices (Institute for Materials Chemistry and Engineering, Kyushu University)". We thank the

OTEC at Saga University and the International Cooperation Projects of Guizhou Province (No. 20137002). The EPSRC is thanked for an overseas travel grant to CR.

Appendix A. Supplementary data

References

[1] X. Zhou, S. Lee, Z. Xu, J. Yoon, Recent progress on the development of chemosensors for gases, Chem. Rev. 115 (2015) 7944–8000.

[2] Y. Zhou, J. Yoon, Recent progress in fluorescent and colorimetric chemosensors for detection of amino acids, Chem. Soc. Rev. 41 (2012) 52–67.

[3] J.F. Zhang, Y. Zhou, J. Yoon, J.S. Kim, Recent progress in fluorescent and colorimetric chemosensors for detection of precious metal ions (silver, gold and platinum ions), Chem. Soc. Rev. 40 (2011) 3416–3429.

[4] J. Wu, W. Liu, J. Ge, H. Zhang, P. Wang, New sensing mechanisms for design of fluorescent chemosensors emerging in recent years, Chem. Soc. Rev. 40 (2011) 3483–3495.

[5] F. Akhgari, H. Fattahi, Y.M. Oskoei, Recent advances in nanomaterial-based sensors for detection of trace nitroaromatic explosives, Sens. Actuators B 221 (2015) 867–878.

[6] J.S. Caygill, F. Davis, S.P.J. Higson, Current trends in explosive detection techniques, Talanta 88 (2012) 14–29.

[7] E. Holmgren, S. Ek, A. Colmsjö, Extraction of explosives from soil followed by gas chromatography–mass spectrometry analysis with negative chemical ionization, J

Chromatogr. A 1222 (2012) 109–115.

[8] C. Cortada, L. Vidal, A. Canals, Determination of nitroaromatic explosives in water samples by direct ultrasound-assisted dispersive liquid–liquid microextraction followed by gas chromatography–mass spectrometry, Talanta 85 (2011) 2546–2552.

[9] S. Schramm, D. Vailhen, M.C. Bridoux, Use of experimental design in the investigation of stir bar sorptive extraction followed by ultra-high-performance liquid chromatography–tandem mass spectrometry for the analysis of explosives in water samples, J. Chromatogr. A 1433 (2016) 24–33.

[10] S. Babaee, A. Beiraghi, Micellar extraction and high performance liquid chromatography-ultra violet determination of some explosives in water samples, Anal. Chim. Acta 662 (2010) 9–13.

[11] J. Lee, S. Park, S.G. Cho, E.M. Goh, S. Lee, S.-S. Koh, J. Kim, Analysis of explosives using corona discharge ionization combined with ion mobility spectrometry–mass spectrometry, Talanta 120 (2014) 64–70.

[12] M. Tabrizchi, V. ILbeigi, Detection of explosives by positive corona discharge ion mobility spectrometry, J. Hazard. Mater. 176 (2010) 692–696.

[13] K.L. Gares, K.T. Hufziger, S.V. Bykov, S.A. Asher, Review of explosive detection methodologies and the emergence of standoff deep UV resonance Raman, J. Raman Spectrosc. 47 (2016) 124–141.

[14] A. Hakonen, P.O. Andersson, M.S. Schmidt, T. Rindzevicius, M. Käll, Explosive and chemical threat detection by surface-enhanced Raman scattering: A review, Anal. Chim. Acta 893 (2015) 1–13.

[15] J. Riedel, M. Berthold, U. Guth, Electrochemical determination of dissolved nitrogen-containing explosives, Electrochimica Acta 128 (2014) 85–90.

[16] J. Zang, C.X. Guo, F. Hu, L. Yu, C.M. Li, Electrochemical detection of ultratrace nitroaromatic explosives using ordered mesoporous carbon, Anal. Chim. Acta 683 (2011) 187–191.

[17] M.S. Meaney, V.L. McGuffin, Investigation of common fluorophores for the detection of nitrated explosives by fluorescence quenching, Anal. Chim. Acta 610 (2008) 57–67.

[18] R. Tu, B. Liu, Z. Wang, D. Gao, F. Wang, Q. Fang, Z. Zhang, Amine-capped $ZnS-Mn^{2+}$ nanocrystals for fluorescence detection of trace TNT, Anal. Chem. 80 (2008) 3458–3465.

[19] M.E. Germain, M.J. Knapp, Optical explosives detection: from color changes to fluorescence turn-on, Chem. Soc. Rev. 38 (2009) 2543–2555.

[20] X. Sun, Y. Wang, Y. Lei, Fluorescence based explosive detection: from mechanisms to sensory materials, Chem. Soc. Rev. 44 (2015) 8019–8061.

[21] R.L. Woodfin, Trace chemical sensing of explosives, John Wiley & Sons, Inc., Hoboken, NJ, USA, 2006, pp. 193–209 (Chapter 9).

[22] S.J. Toal, W.C. Trogler, Polymer sensors for nitroaromatic explosives detection, J. Mater. Chem. 16 (2006) 2871–2883.

[23] Z. Hu, B.J. Deibert, J. Li, Luminescent metal–organic frameworks for chemical sensing and explosive detection, Chem. Soc. Rev. 43 (2014) 5815–5840.

[24] S. Shanmugaraju, P.S. Mukherjee, π-Electron rich small molecule sensors for the

recognition of nitroaromatics, Chem. Commun. 51 (2015) 16014–16032.

[25] Y. Salinas, R. Martínez-Máñez, M.D. Marcos, F. Sancenón, A.M. Costero, M. Parra, S. Gil, Optical chemosensors and reagents to detect explosives, Chem. Soc. Rev. 41 (2012) 1261–1296.

[26] R. Joseph, C.P. Rao, Ion and molecular recognition by lower rim 1,3-di-conjugates of calix[4]arene as receptors, Chem. Rev. 111 (2011) 4658–4702.

[27] J.S. Kim, D.T. Quang, Calixarene-derived fluorescent probes, Chem. Rev. 107 (2007) 3780−3799.

[28] H.C. Kolb, M.G. Finn, K.B. Sharpless, Click chemistry: diverse chemical function from a few good reactions, Angew. Chem. Int. Ed. 40 (2001) 2004–2021.

[29] J.J. Bryant, U.H.F. Bunz, Click to bind: metal sensors, Chem. Asian J. 8 (2013) 1354–1367.

[30] Y.H. Lau, P.J. Rutledge, M. Watkinson, M.H. Todd, Chemical sensors that incorporate click-derived triazoles, Chem. Soc. Rev. 40 (2011) 2848–2866.

[31] M. Song, Z. Sun, C. Han, D. Tian, H. Li, J.S. Kim, Calixarene-based chemosensors by means of click chemistry, Chem. Asian J. 9 (2014) 2344–2357.

[32] D. Schweinfurth, S. Strobel, B. Sarkar, Expanding the scope of ‘Click’ derived 1,2,3-triazole ligands: New palladium and platinum complexes, Inorg. Chim. Acta 374 (2011) 253–260.

[33] D. Urankar, A. Pevec, I. Turel, J. Košmrlj, Pyridyl conjugated 1,2,3-triazole is a versatile coordination ability ligand enabling supramolecular associations, Cryst. Growth Des. 10 (2010) 4920–4927.

[34] B. Gole, S. Shanmugaraju, A.K. Bara, P.S. Mukherjee, Supramolecular polymer for explosives sensing: role of H-bonding in enhancement of sensitivity in the solid state, Chem. Commun. 47 (2011) 10046–10048.

[35] X.L. Ni, S. Wang, X. Zeng, Z. Tao, T. Yamato, Pyrene-linked triazole-modified homooxacalix[3]arene: a unique C_3 symmetry ratiometric fluorescent chemosensor for Pb^{2+}, Org. Lett. 13 (2011) 552–555.

[36] C. Wu, Y. Ikejiri, J.L. Zhao, X.K. Jiang, X.L. Ni, X. Zeng, C. Redshaw, T. Yamato, A pyrene-functionalized triazole-linked hexahomotrioxacalix[3]arene as a fluorescent chemosensor for Zn^{2+} ions, Sens. Actuators B 228 (2016) 480–485.

[37] M.K. Chahal, M. Sankar, 1,8-Naphthyridine-based fluorescent receptors for picric acid detection in aqueous media, Anal. Methods 7 (2015) 10272–10279.

[38] S.S. Nagarkar, A.V. Desai, S.K. Ghosh, A fluorescent metal–organic framework for highly selective detection of nitro explosives in the aqueous phase, Chem. Commun. 50 (2014) 8915–8918.

[39] V. Bhalla, H. Arora, H. Singh, M. Kumar, Triphenylene derivatives: chemosensors for sensitive detection of nitroaromatic explosives, Dalton Trans. 42 (2013) 969–974.

[40] S. Shanmugaraju, P.S. Mukherjee, Self-assembled discrete molecules for sensing nitroaromatics, Chem. Eur. J. 21 (2015) 6656–6666.

[41] Y.H. Lee, H. Liu, J.Y. Lee, S.H. Kim, S.K. Kim, J.L. Sessler, Y. Kim, J.S. Kim, Dipyrenylcalix[4]arene–a fluorescence-based chemosensor for trinitroaromatic explosives, Chem. Eur. J. 16 (2010) 5895–5901.

[42] B. Joarder, A.V. Desai, P. Samanta, S. Mukherjee, S.K. Ghosh, Selective and sensitive aqueous-phase detection of 2,4,6-trinitrophenol (TNP) by an amine-functionalized metal–organic framework, Chem. Eur. J. 21 (2015) 965–969.

[43] S.S. Nagarkar, B. Joarder, A.K. Chaudhari, S. Mukherjee, S.K. Ghosh, Highly selective detection of nitro explosives by a luminescent metal–organic framework, Angew. Chem. Int. Ed. 52 (2013) 2881–2885.

[44] R. Chopra, P. Kaur, K. Singh, Pyrene-based chemosensor detects picric acid upto attogram level through aggregation enhanced excimer emission, Anal. Chim. Acta 864 (2015) 55–63.

[45] S. Hussain, A.H. Malik, M.A. Afroz, P.K. Iyer, Ultrasensitive detection of nitroexplosive – picric acid via a conjugated polyelectrolyte in aqueous media and solid support, Chem. Commun. 51 (2015) 7207–7210.

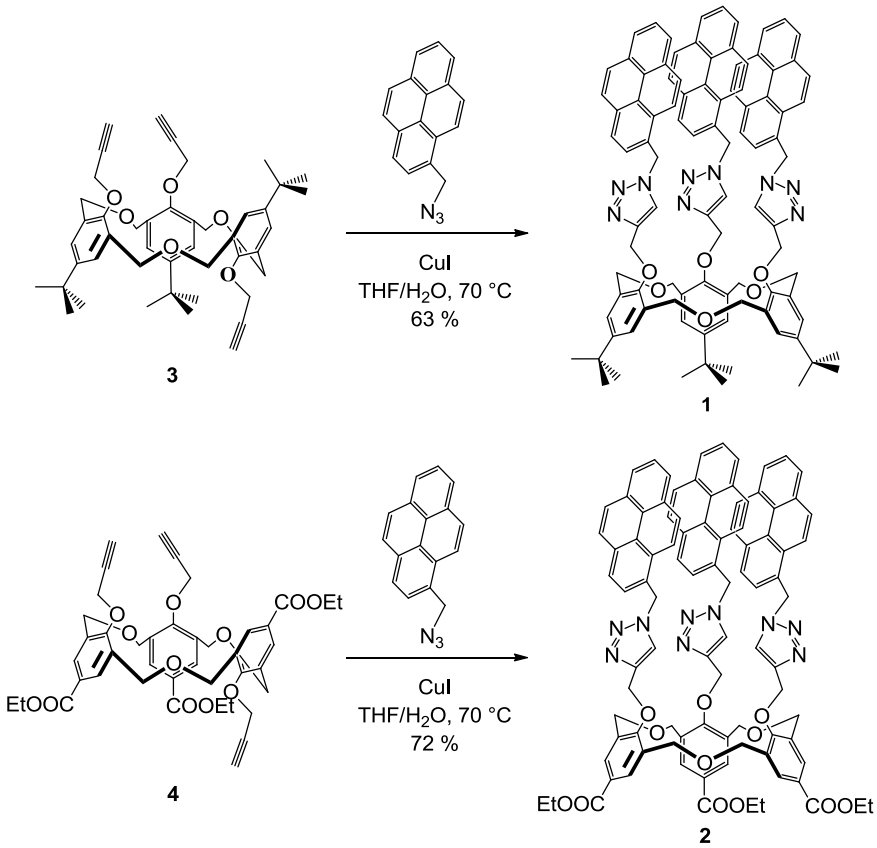

Scheme 1 The synthetic route of chemosensors **1** and **2**.

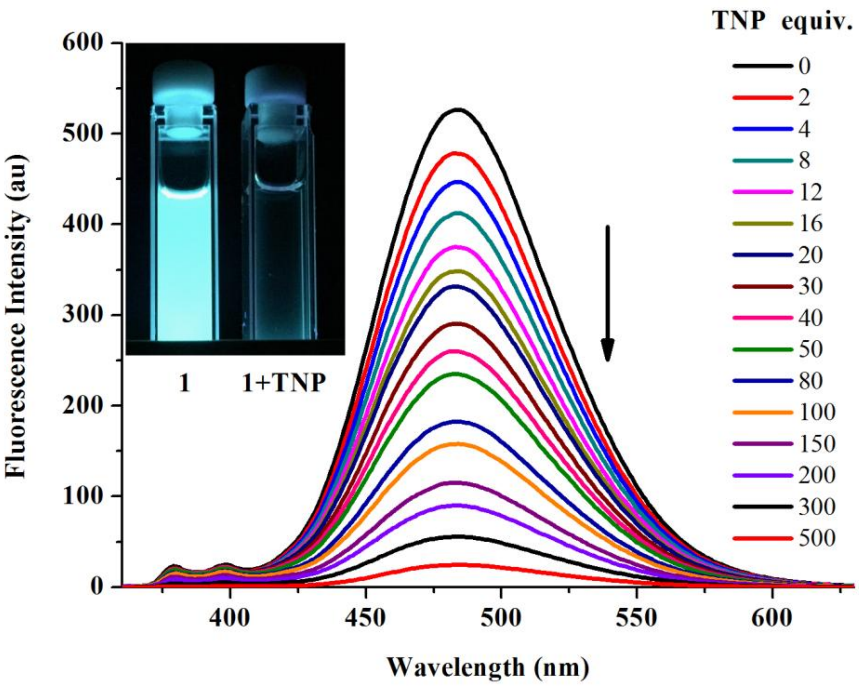

Fig. 1 Fluorescence emission spectra of **1** (1.0 μM) upon the addition of increasing concentrations of TNP in CH_3CN. λ_{ex} = 343 nm. The inset shows the fluorescence color of **1** before and after the addition of TNP.

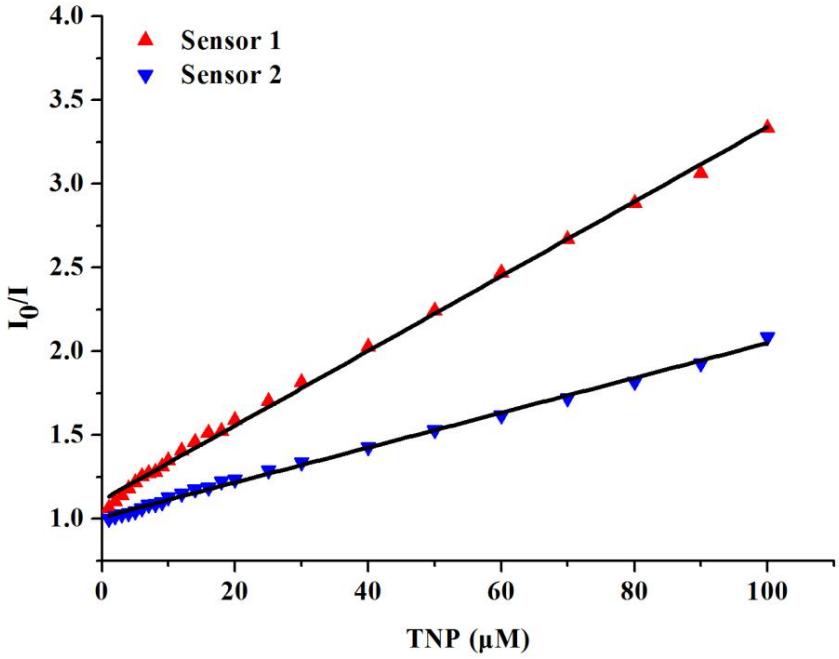

Fig. 2 Stern–Volmer plots for the titration of sensors **1** and **2** with TNP at lower concentrations (up to 100 μM).

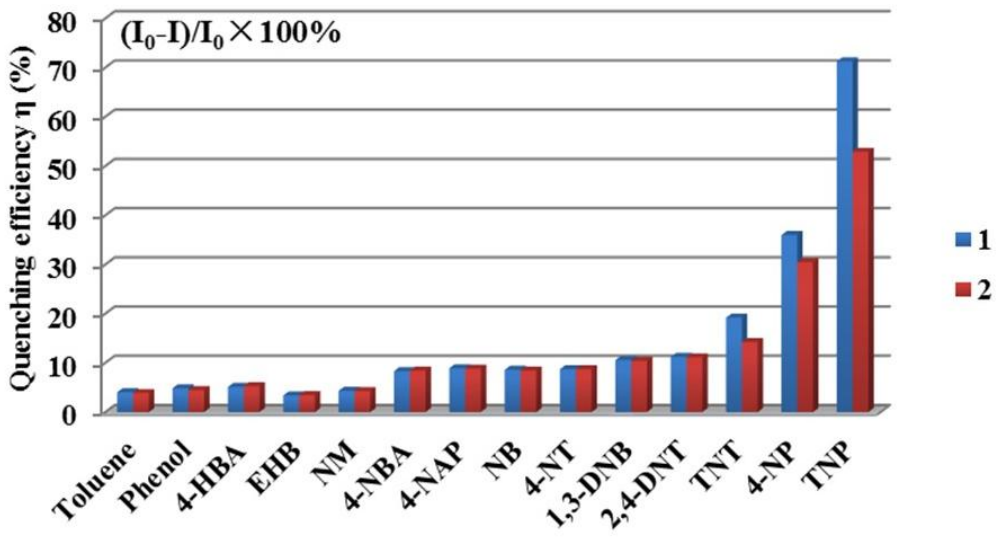

Fig. 3 Reduction in fluorescence intensity (plotted as quenching efficiency) seen upon the addition of 100 equiv. of analytes. 4-HBA = 4-hydroxybenzoic acid, EHB = ethyl 4-hydroxybenzoate, NM = nitromethane, 4-NBA = 4-nitrobenzoic acid, 4-NAP = 4-nitroacetophenone, NB = nitrobenzene, 4-NT = 4-nitrotoluene, 1,3-DNB = 1,3-dinitrobenzene, 2,4-DNT = 2,4-dinitrotoluene, TNT = 2,4,6-trinitrotoluene, 4-NP = 4-nitrophenol and TNP = 2,4,6-trinitrophenol.

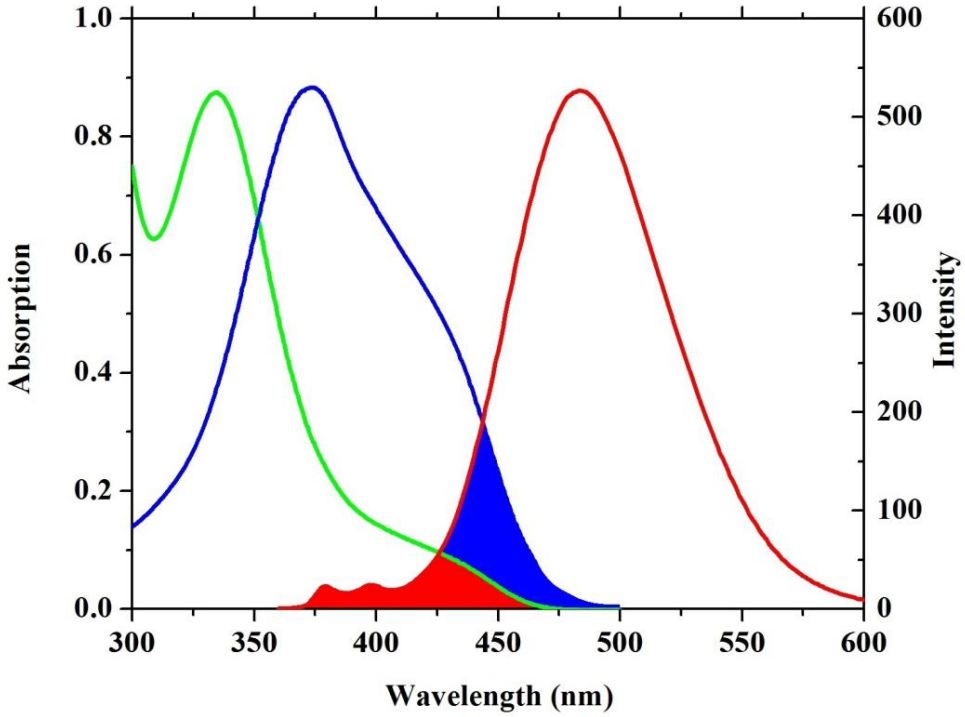

Fig. 4 Spectral overlaps between absorption spectra of TNP (green line), TNP in the presence of amine (blue line) and the emission spectrum of **1** (red line).

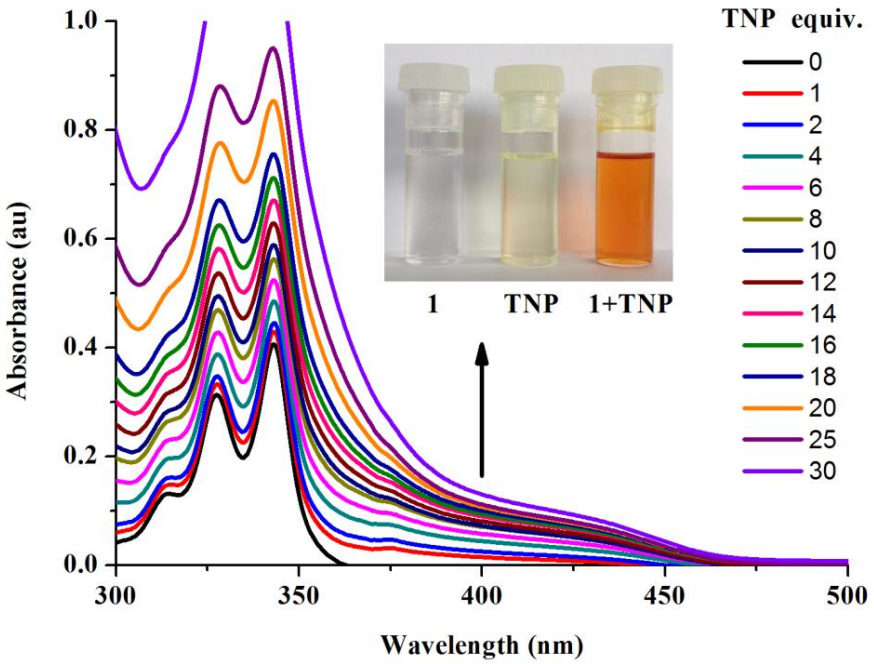

Fig. 5 Change in absorption spectra of sensor **1** (5.0 μM) with the addition of TNP in CH_3CN. Inset: visual colour change due to the formation **1**•TNP complex.

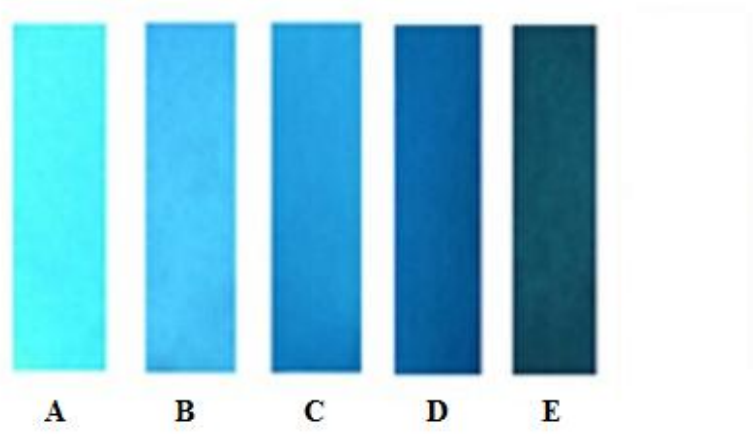

Fig. 6 Photographs (under 365 nm UV light) of the fluorescence response of **1** on test strips after contact with various concentrations of TNP: (A) 0.0 μM, (B) 5.0 μM, (C) 10.0 μM, (D) 100.0 μM and (E) 0.5 mM.

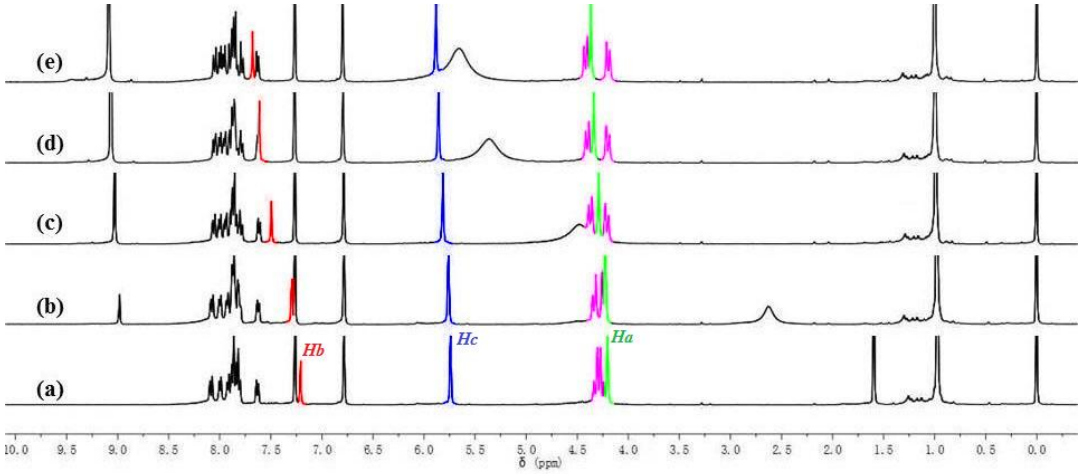

Fig. 7 The ^{1}H NMR spectra of **1** (5.0 mM) upon titration with TNP in $CDCl_3$. (a) **1** only, (b c d and e) in the presence of 1.0, 5.0, 10.0 and 15.0 equiv. of TNP, respectively.

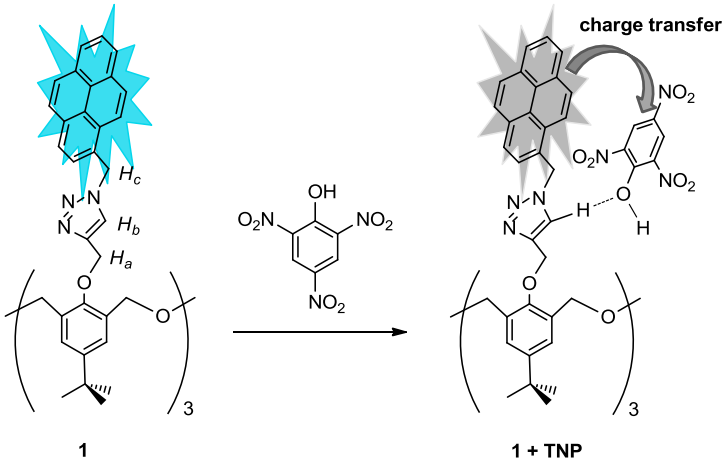

Fig. 8 Plausible binding mode between **1** and TNP.